

X-RAYS FROM MAGNETIC FLARES IN CYGNUS X-1: THE ROLE OF A TRANSITION LAYER

SERGEI NAYAKSHIN¹ AND JAMES B. DOVE²

¹Physics Department, The University of Arizona, Tucson AZ 85721

²CASA, University of Colorado, Boulder, CO 80309

Draft version September 3, 2018

ABSTRACT

The spectrum of Seyfert 1 Galaxies is very similar to that of several Galactic Black Hole Candidates (GBHCs) in their hard state, suggestive that both classes of objects have similar physical processes. While it appears that an accretion disk corona (ADC) model, where the corona sandwiches the cold accretion disk, is capable of explaining the observations of Seyfert galaxies, recent work has shown that this model is problematic for GBHCs. To address the differences in the spectra of Seyferts and GBHCs, we consider the structure of the atmosphere of the accretion disk in a region near an active magnetic flare (we refer to this region as transition layer). We show that the transition layer is subject to a thermal instability, similar in nature to the ionization instability of quasar emission line regions. We find that due to the much higher ionizing X-ray flux in GBHCs, the only stable solution for the upper layer of the accretion disk is that in which it is highly ionized and is at the Compton temperature ($kT \sim$ a few keV). Using numerical simulations for a slab geometry ADC, we show that the presence of a transition layer, here modeled as being completely ionized, can significantly alter the spectrum of escaping radiation for modest optical depths. Due to the higher albedo of the disk, the transition layer leads to a reduction in reprocessing features, i.e., the iron line and the X-ray reflection hump. In addition, if most of the accretion energy is dissipated in the corona, the thermal blackbody component is reduced, giving rise to a lower Compton cooling rate within the corona. Although a transition layer does allow for higher coronal temperatures, global two-phase, slab-geometry ADC models still cannot have coronal temperatures high enough to explain the data unless the optical depth of the transition layer is unphysically large ($\gtrsim 10$). However, a model having a patchy corona rather than a global corona appears promising. Thus, it is possible that due to the thermal instability of the surface of the accretion disk, which leads to different endpoints for GBHCs and Seyfert galaxies, the X-ray spectra from these two types of objects can be explained by a single unifying ADC model.

Subject headings: accretion disks — black hole physics — Cygnus X-1 — galaxies: Seyfert — magnetic fields — radiative transfer

1. INTRODUCTION

The X-ray spectra of Seyfert Galaxies and Galactic Black Hole Candidates (GBHCs) indicate that the reflection and reprocessing of incident X-rays into lower frequency radiation is an ubiquitous and important process. For Seyfert Galaxies, the X-ray spectral index hovers near a “canonical value” (~ 0.95 ; Pounds et al. 1990, Nandra & Pounds 1994; Zdziarski et al. 1996, but also see Brandt & Boller 1998), after the reflection component has been subtracted out of the observed spectrum. It is generally believed that the universality of this X-ray spectral index may be attributed to the fact that the reprocessing of X-rays within the cold accretion disk leads to an electron cooling rate that is roughly proportional to the heating rate inside the active regions (AR) (Haardt & Maraschi 1991, 1993; Haardt, Maraschi & Ghisellini 1994; Svensson 1996).

Although the X-ray spectra of GBHCs are similar to that of Seyfert galaxies, they are considerably harder (most have a power-law index of $\Gamma \sim 0.7$), and the reprocessing features are less prominent (Zdziarski et al. 1996, Dove et al. 1997). It is the relatively hard power law (and therefore the required large coronal temperature) and the weak reprocessing/reflection features that led Dove et al. (1997, 1998), Gierlinski et al. (1997) and Poutanen, Krolik & Ryde (1997) to conclude that the two-phase accretion disk corona (ADC) model, in both patchy and slab corona geometry cases, does not apply to Cygnus X-1.

One of the main problems with the global slab-geometry ADC model is that, for a given coronal optical depth, no self-

consistent coronal temperature is high enough to produce a spectrum both as hard and with an exponential cutoff at an energy as high as that of Cyg X-1 (Dove, Wilms, & Begelman 1997). However, this result is sensitive to the assumption that the accretion disk is relatively cold, such that $\sim 90\%$ of the reprocessed coronal radiation is re-emitted by the disk as thermal radiation (with a temperature ~ 150 eV). It is this thermal radiation that dominates the Compton cooling rate within the corona. If the upper layers of the accretion disk were highly ionized, creating a “transition layer,” a smaller fraction of the incident coronal radiation would be reprocessed into thermal radiation (i.e., the albedo of the disk would be increased), and therefore the Compton cooling rate in the corona would be reduced. Furthermore, as shown by Ross, Fabian & Brandt (1996; RFB96 hereafter), the high ionization state of the outer atmosphere of the accretion disk in GBHCs may explain the weakness of observed iron line features in Cyg X-1.

Recently, Nayakshin & Melia (1997) investigated (via simple qualitative considerations) the structure of the X-ray reflecting material in AGNs assuming that the ARs are magnetic flares above the disk (Haardt et al. 1994; see also Galeev, Rosner & Vaiana 1979). They showed that the pressure and energy equilibrium conditions for the X-ray illuminated upper layer of the disk require the gas temperature to be $T \sim \text{few} \times 10^5$ K, leading the upper atmosphere of the disk to a low ionization state.

In this paper, we consider the reprocessing of X-rays from ARs for GBHCs. In §2, we show that there should be a thermal instability at the surface of the cold disk, causing the temper-

ature to climb up to $T \sim$ a few $\times 10^7$ K. This temperature is roughly the Compton temperature with respect to the coronal radiation field. At this temperature the transition layer turns out to be almost completely ionized. Recently, Böttcher, Liang, and Smith (1998), using an iterative method, a linear Comptonization algorithm, and the photoionization model XSTAR, also found that a highly ionized transition layer should form for moderate ionization parameters, i.e., ionization parameters thought to be appropriate for GBHCs. In §3, we explore the ramifications of this highly ionized transition layer on the energetics of the corona, and investigate how it alters the spectrum of escaping radiation. We also discuss whether slab geometry ADC models, when transition layers are included, can account for the observed spectra of BHCs. In §4, we give our conclusions.

2. THE FORMATION OF A TRANSITION LAYER

2.1. Physical Conditions in X-ray Skin Near Magnetic Flares

The two-phase model was put forward by Haardt & Maraschi (1991, 1993) to explain the spectra of Seyfert Galaxies. Haardt et al. (1994) pointed out that observations are inconsistent with a uniform corona and introduced a patchy corona, where each “patch” is a magnetic flare (also referred as an active region). The key assumptions of the model are (1) during the flare, the X-ray flux from the active region greatly exceeds the disk intrinsic flux, and (2) the compactness parameter l of the active region is large, so that the dominant radiation mechanism is Comptonization of the disk thermal radiation. We wish to apply the same model to the X-ray spectra of GBHCs, and we employ the same assumptions.

As discussed below, we argue for the existence of a transition layer in the vicinity of an active coronal region (see Figure 1). Since the flux of ionizing radiation is proportional to $1/d^2 \times \cos i \propto d^{-3}$, where i is the angle between the normal of the disk and the direction of the incident radiation field and d is the distance between the active region and the position on the disk, the ionization state of the disk surface will vary across the disk. Consequently, only the gas near the active regions (with a radial size \sim a few times the size of the active region, situated directly below it) may be highly ionized. Most reprocessing of coronal radiation will take place in the transition regions; in addition, most radiation emitted by the disk that propagates through the active regions will have been emitted in the vicinity of the transition regions. Therefore, in this paper, we will only consider a one-zone model, consisting of the active region, the transition layer, and the underlying cold disk.

The structure of the transition layer, i.e., its temperature, density and ionization state are determined by solving the energy, ionization and pressure balance conditions. The first two conditions have been extensively treated in the literature, and we will follow these standard methods here (see §2.2). The pressure equilibrium condition is typically replaced by the constant gas density assumption (e.g., RFB, Zycki et al. 1994 and references therein). For the problem at hand, however, the equilibrium state of the transition layer is sensitive to the pressure balance, and thus we will attempt to take it into account. Accounting for the pressure balance leads to results that are substantially different from previous work, as discussed below.

The X-ray radiation pressure on the transition layer is equal to F_x/c , where F_x is the flux produced by the magnetic flare.

The compactness parameter of the active region, l , is defined as

$$l \equiv \frac{F_x \sigma_T \Delta R}{m_e c^3}, \quad (1)$$

and is expected to be larger than unity (e.g., Poutanen & Svensson 1996, Poutanen, Svensson & Stern 1997). The size of the active region ΔR is thought to be of the order of the accretion disk height scale H (e.g., Galeev et al. 1979). Here, H/R is estimated from the gas pressure dominated solution of Svensson & Zdziarski (1994; SZ94 hereafter),

$$\frac{H}{R} = 7.5 \times 10^{-3} (\alpha M_1)^{-1/10} r^{1/20} [\dot{m} J(r)]^{1/5} [(1-f)]^{1/10}, \quad (2)$$

where α is the viscosity parameter, $M_1 \equiv M/10 M_\odot$ is the mass of the black hole, f is the fraction of accretion power dissipated into the corona (averaged over the whole disk), r is the radius relative to the Schwarzschild radius ($r \equiv R/R_g$), $J(r) = 1 - (3/r)^{1/2}$. For the case of the hard state of Cyg X-1, most of the bolometric luminosity is in the hard X-ray band (e.g., Gierlinski et al. 1997). Thus, most of the accretion energy must be dissipated directly in the corona, i.e., $f \sim 1$ (Haardt and Maraschi 1991; Stern et al. 1995). The dimensionless accretion rate $\dot{m} = \eta \dot{M} c^2 / L_{\text{Edd}}$ for Cyg X-1 seems to be around 0.05. Here, \dot{M} is the accretion rate, $\eta = 0.056$ is the efficiency for the standard Shakura-Sunyaev disk, and L_{Edd} is the Eddington luminosity. Note that this definition of \dot{m} is different by factor η from that used by SZ94 (i.e., $\dot{m} \simeq 17 \times \dot{m}_{\text{SZ94}}$). Finally, for $r = 6$, the X-ray flux is

$$F_x \simeq 4 \times 10^{23} l \alpha^{1/10} M_1^{-9/10} \left(\frac{\dot{m}}{0.05} \right)^{-1/5} (1-f)^{-1/10} \text{erg cm}^{-2} \text{sec}^{-1} \quad (3)$$

To check whether assumption (1) of the patchy two-phase model is consistent for Cyg X-1 parameters, we estimate the intrinsic flux of the disk,

$$F_d = 1.0 \times 10^{22} M_1^{-1} \left(\frac{\dot{m}}{0.05} \right) (1-f) \text{erg cm}^{-2} \text{sec}^{-1}. \quad (4)$$

It is seen that the X-ray flux is indeed much larger than the intrinsic disk emission if $1-f \ll 1$ and the compactness parameter $l \gg 0.01$.

The pressure of the disk surface layer before the occurrence of a flare (or, equivalently, far enough from the flare), assuming that the upper layer of the disk with Thomson optical depth $\tau_x \sim$ few is in the hydrostatic equilibrium, is

$$P_0 \simeq \frac{GMm_p}{R^2} \tau_x \frac{H}{R} = 6.2 \times 10^{10} M_1^{-11/10} \alpha^{-1/10} \times \tau_x \left(\frac{\dot{m}}{0.05} \right)^{1/5} (1-f)^{1/10} \text{erg cm}^{-3}, \quad (5)$$

where $r = 6$ (SZ94). Near an active magnetic flare, the ratio of the incident radiation pressure to the unperturbed accretion disk atmosphere pressure is

$$\frac{F_x}{cP_0} = 2. \times 10^2 l \tau_x^{-1} (\alpha M_1)^{1/5} \left(\frac{\dot{m}}{0.05} \right)^{-2/5} (1-f)^{-1/5}, \quad (6)$$

Since the radiation pressure from the active region greatly exceeds the unperturbed thermal pressure, the transition layer will contract until the gas pressure P

$$P \sim F_x/c. \quad (7)$$

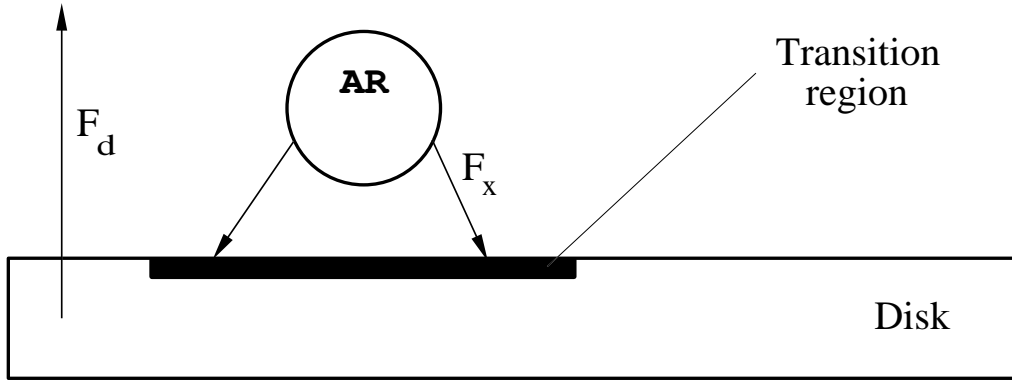


Fig. 1.— The geometry of the active region (AR: magnetic flare) and the transition layer. Magnetic fields, containing AR and supplying it with energy are not shown. Transition region is defined as the upper layer of the disk with Thomson depth of \sim few, where the incident X-ray flux is substantially larger than the intrinsic disk flux

A better treatment would solve for the gas opacity in the transition layer and thus the radiation force self-consistently, rather than simply using the ram pressure F_x/c (Nayakshin 1998). However, inequality (7) turns out to be sufficient to prove the main point of this paper. We thus move on to solve the energy and ionization balance equations for the transition layer.

2.2. The Thermal Instability

A general condition for a thermal instability was discovered by Field (1965). He argued that a physical system is usually in pressure equilibrium with its surroundings. Thus, any perturbations of the temperature T and the density n of the system should occur at a constant pressure. The system is unstable when

$$\left(\frac{\partial \Lambda_{\text{net}}}{\partial T}\right)_P < 0, \quad (8)$$

where the “cooling function,” Λ_{net} , is the difference between cooling and heating rates per unit volume, divided by the gas density n squared.

In ionization balance studies, it turns out convenient to define two parameters. The first one is the “density ionization parameter” ξ , equal to (Krolik, McKee & Tarter 1981)

$$\xi = \frac{4\pi F_x}{n}, \quad (9)$$

The second one is the “pressure ionization parameter”, defined as

$$\Xi \equiv \frac{P_{\text{rad}}}{P}, \quad (10)$$

where P is the full isotropic pressure due to neutral atoms, ions, electrons and the trapped line radiation. (This definition of Ξ is the one used in the ionization code XSTAR, and is more appropriate for studies of the instabilities than the original definition of Ξ given in Krolik et al. 1981, who used nkT instead of the full pressure P . For temperatures typical of GBHCs, however, we found that the trapped line radiation was always a small fraction, e.g., \sim few percent of the total pressure, and therefore the two definitions of Ξ are nearly identical). Krolik et al. (1981) showed that the instability criterion (8) is equivalent to

$$\left(\frac{d\Xi}{dT}\right)_{\Lambda_{\text{net}}=0} < 0, \quad (11)$$

where the derivative is taken with the condition $\Lambda_{\text{net}} = 0$ satisfied, i.e., when the energy balance is imposed. In this form,

the instability can be easily seen when one plots temperature T versus Ξ .

We now apply the X-ray ionization code XSTAR (Kallman & McCray 1982, Kallman & Krolik 1986), to the problem of the transition layer. A truly self-consistent treatment would involve solving radiation transfer in the optically thick transition layer, and, in addition, finding the distribution of the gas density in the transition layer that would satisfy pressure balance. Since radiation force acting on the gas depends on the opacity of the gas, this is a difficult non-linear problem. Thus, we defer such a detailed study to future work, and simply solve (using XSTAR) the local energy and ionization balance for an *optically thin layer* of gas in the transition region. We assume that the ionizing spectrum consists of the incident X-ray power law with the energy spectral index typical of GBHCs in the hard state, i.e., $\Gamma = 1.5 - 1.75$, exponentially cutoff at 100 keV, and the blackbody spectrum from the cold disk below the transition layer. If the energy and ionization balance is found to be unstable for this setup, the transition layer will also be unstable, because the instability is local in character.

Note that it is not possible for the transition region to have a temperature lower than the effective temperature of the X-radiation, i.e., $T_{\text{min}} = (F_x/\sigma)^{1/4}$. The reason why the simulations may give temperatures lower than T_{min} for low values of ξ is that in this parameter range XSTAR neglects certain non-radiative de-excitation processes, which leads to an overestimate of the cooling rate (Zycki et al. 1994; see their section 2.3). Since we are using a one-zone model for the transition layer, we use an attenuated X-ray flux $\langle F_x \rangle$ which represents the surface-averaged value as seen by the transition region, $\langle F_x \rangle = F_x/b = 0.1F_x/b_1$, where b is a dimensionless number of order 10, $b_1 = b/10$, and F_x is the X-ray flux leaving the active region (see figure 1). Using equation (3),

$$T_{\text{min}} \simeq 5.0 \times 10^6 l^{1/4} b_1^{-1/4} \left(\frac{\dot{m}}{0.05}\right)^{-1/20} \alpha^{1/40} M_1^{-9/40} [1-f]^{-1/40} \quad (12)$$

Figure 2 shows results of our calculations for several different X-ray ionizing spectra. A stable solution for the transition layer structure will have a positive slope, and also satisfy the pressure equilibrium condition. As discussed in §2.1, $P \leq F_x/c$ (i.e., $\Xi \geq 1$). In addition, if the gas is completely ionized, the absorption opacity is negligible compared to the

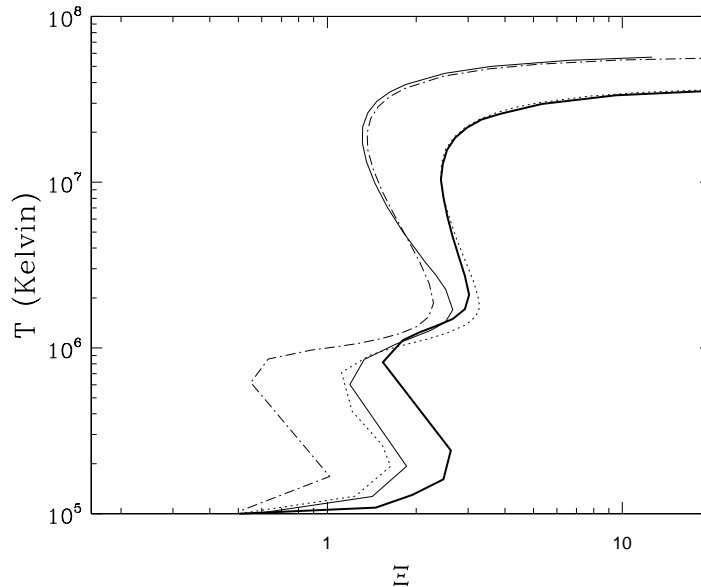


Fig. 2.— Gas temperature versus pressure ionization parameter Ξ – the ionization equilibrium curves for parameters appropriate for GBHCs. The incident spectrum is approximated by a power law of photon index Γ , exponentially cutoff at 100 keV, and the reflected blackbody with equal flux and temperature T_{\min} (equation 12). Values of the parameters are: $\Gamma = 1.5, 1.75, 1.75, 1.7$ and $kT_{\min} = 200, 100, 200, 400$ eV, corresponding to the fine solid, thick solid, dotted and dash-dotted curves, respectively. Because the ionization equilibrium is unstable when the curve has a negative slope, and because there exists no solution below T_{\min} (see text), the only stable solution is the uppermost branch of the curve with $T \gtrsim 10^7$ K.

Thomson opacity. Because all the incident X-ray flux is eventually reflected, the net flux is zero, and so the net radiation force is zero (note that the momentum of the incident radiation is reflected deep inside the disk, so the radiation does apply a ram pressure equal to $2F_x/c$ to the whole disk, but *not to the transition layer*). In that case the pressure P adjusts to the value appropriate for the accretion disk atmosphere in the absence of the ionizing flux (see also Sincell & Krolik 1996), which is given by equation (5). Therefore, the pressure ionization parameter should be in the range

$$1 < \Xi < 1 \times 10^2 l (\alpha M_1)^{1/5} \left(\frac{\dot{m}}{0.05} \right)^{2/5} (1-f)^{-1/5}. \quad (13)$$

With respect to the ionization equilibria shown in Figure (2), the gas is almost completely ionized on the upper stable branch of the solution (i.e., the one with $T \gtrsim 10^7$ K), and thus the pressure equilibrium for such temperatures requires $\Xi \sim F_x/cP_0 \gg 1$, which is allowed according to equation (13).

In addition to the stable Compton equilibrium state, there is a small range in parameter space, with the temperature between 100 and 200 eV, in which a stable thermal state exists. The presence of this region is explained by a rapid decrease in *heating* (with T increasing), rather than an increase in cooling (cf. equation 8). The X-ray heating rate decreases in the temperature range 100 – 200 eV with increasing T since higher temperatures lead to higher ionization rates of ion species with ionization energies $\sim kT$. This larger degree of ionization reduces the X-ray opacity, and thus the heating rate as well. Note that it is highly unlikely that the transition region will stabilize within the temperature range 100 – 200 eV because the effective temperature, T_{\min} , is most likely above this temperature range.

Due to the above considerations, it is very likely that the tran-

sition layer is highly ionized in GBHCs *in the hard state* for $\tau_x \lesssim 1$. The upper limit of τ_x can only be found by a more exact treatment. In addition, the transition layer may be heated by the same process that heats the corona above it, albeit with a smaller heating rate. Furthermore, Maciolek-Niedzwiecki, Krolik & Zdziarski (1997) have recently shown that the thermal conduction of energy from the corona to the disk below may become important for low coronal compactness parameters and substantially contribute to the heating rate of the transition layer. Thus, the transition layer may be even hotter than found by photoionization calculations.

Eventually, the X-rays are down-scattered and the radiation spectrum becomes softer as one descends from the top of the transition layer to its bottom. We can qualitatively test the gas ionization stability properties by allowing the ionizing spectrum to be softer than the observed spectrum of GBHCs in the hard state. In Figure 3 we show two examples of such calculations. The slope of the ionization equilibrium curve becomes positive everywhere above $kT \sim 100$ eV, so that these equilibria are stable, and thus the gas temperature may saturate at $T \sim T_{\min}$, far below few keV, the appropriate temperature for the uppermost layer of the transition region. Thus, we know (see also §4) that the transition layer should terminate at some value of $\tau_x \sim \text{few}$.

We point out the similarity of our results to those of Krolik, McKee & Tarter (1981) for the emission line regions in quasars. These authors solved the ionization and energy balance equations for optically thin clouds illuminated by a broad band quasar spectrum, and showed that the thermal instability exists if the pressure ionization parameter is close to unity. They found that there are two stable states for the line emitting clouds, one cold and one hot. The cold state corresponds to the gas temperature $T \lesssim \text{few} \times 10^4$ K, where collisional cooling balances ionization heating. The hot state corresponds to tem-

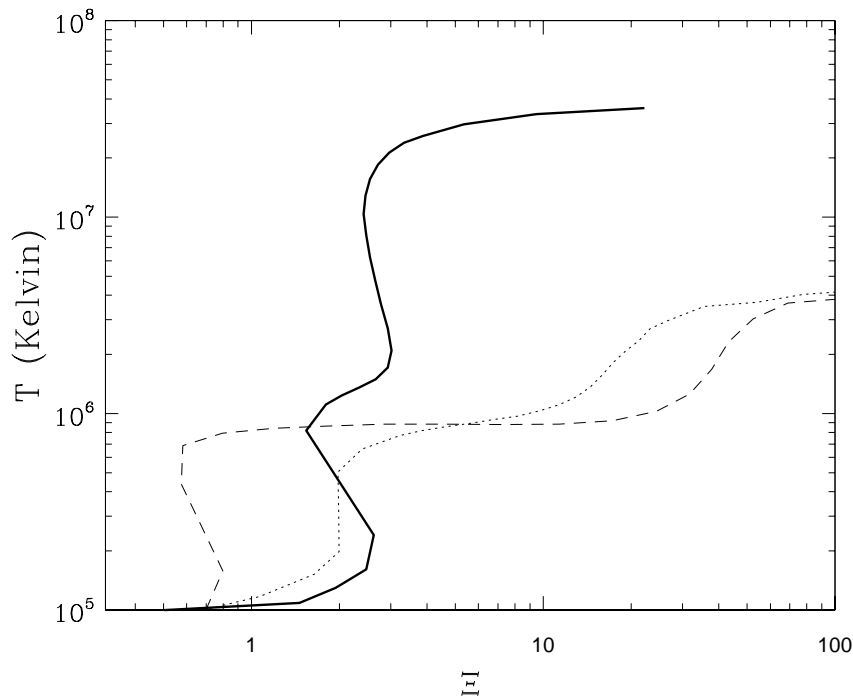


Fig. 3.— Same as Figure 2. The thick solid curve is same as that in Figure 2 and is appropriate for the hard state of a GBHC, whereas two other curves are relevant to the soft state in GBHCs, or at large depth in the transition layer (see Discussion). Values of the parameters are: $\Gamma = 2.1, 2.1$ and $kT_{\text{min}} = 200, 400$ eV for the dotted and dashed curves, respectively.

peratures $T \gtrsim 10^7$ K, when ionization heating decreases due to almost complete ionization of the elements and the Compton heating decreases since the gas is close to the Compton temperature T_{comp} . Here, we found a similar instability for the X-ray skin near an active magnetic flare in accretion disks of GBHCs. The lower temperature equilibrium state is not allowed, however, since the gas density and the X-ray ionizing flux in GBHCs is larger than these quantities in quasar emission line regions by some $\sim 10 - 12$ orders of magnitude. Finally, we note that the thermal instability is not apparent in studies where the gas density is fixed to a constant value. Following Field (1965), we argue that the assumption of the constant gas density is not justified for real physical systems, and that one always should use the pressure equilibrium arguments to determine the actual gas density and the stability properties of the system.

3. GLOBAL ADC MODELS WITH A TRANSITION LAYER

3.1. Physical Setup

We now explore how a transition layer affects the physical properties of the coronal gas and the spectrum of escaping radiation. Since a transition layer may occur for both a global ADC model and for a patchy coronal model, both models should be explored in detail. In this paper, however, we only study the global ADC model, and defer a self-consistent treatment of the patchy corona to a future paper. We expect, however, that the systematic trends found for the global ADC models should also occur for the patchy model, with the main difference being the maximum coronal temperature of the patchy model being higher.

A self consistent treatment of the transition layer would solve for the ionization layer structure as a function of optical depth. However, we will make the simplifying assumption that the transition layer is completely ionized. The optical depth of the

transition layer will be kept as a free parameter, and we will explore how sensitive the spectrum of escaping radiation is to τ_{tr} . The two issues we will address are (1) for a given coronal optical depth (e.g., one thought to be appropriate for fitting the spectra of GBHCs), how does the maximum coronal temperature depend on the optical depth of the transition layer, and (2) how does the spectrum of escaping radiation, most importantly the reprocessing features, vary with the optical depth of the transition layer. Of particular importance is the parameter range of τ_{tr} such that the predicted spectrum is consistent with that of GBHCs, and whether these values of τ_{tr} are consistent with the assumption of the transition layer being completely ionized.

The model contains three regions: (1) A cold accretion disk, assumed here to have a temperature $kT_{\text{bb}} = 150$ keV, (2) the transition layer, situated directly above the cold disk, and (3) the corona, situated directly above the transition layer. Plane parallel geometry is assumed.

We use the slab-geometry ADC model of Dove, Wilms, & Begelman (1997), which uses a non-linear Monte Carlo (NLMC) routine to solve the radiation transfer problem of the system. The free parameters of the model are the seed optical depth τ_e , (the optical depth of the corona excluding the contribution from electron-positron pairs), the blackbody temperature of the accretion disk and its compactness parameter, l_{bb} , and the heating rate (i.e., the compactness parameter), l_c , of the ADC. The temperature structure of the corona is determined numerically by balancing Compton cooling with heating, where the heating rate is assumed to be uniformly distributed. The e^-e^+ -pair opacity is given by balancing photon-photon pair production with annihilation. Reprocessing of coronal radiation in the cold accretion disc is also treated numerically. For a more thorough discussion of the NLMC routine, see Dove, Wilms, &

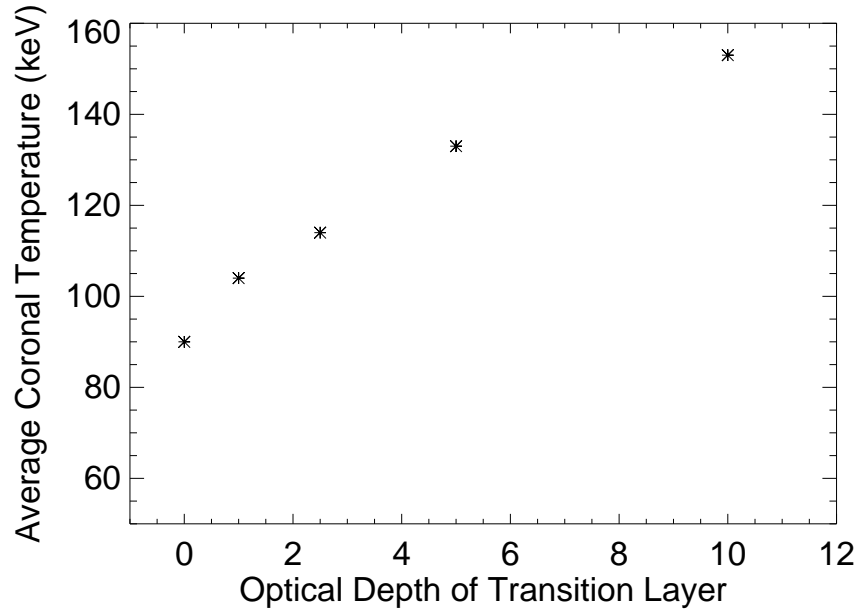


Fig. 4.— The maximum temperature of the corona as a function of the optical depth of the transition layer. For all models, we assume that the intrinsic compactness parameter of the disk is $l_{\text{bb}} = 0.01$ and the disk temperature is $kT_{\text{bb}} = 150$ eV. For all models, the maximum temperature is reached for $l_c \sim 2 - 5$.

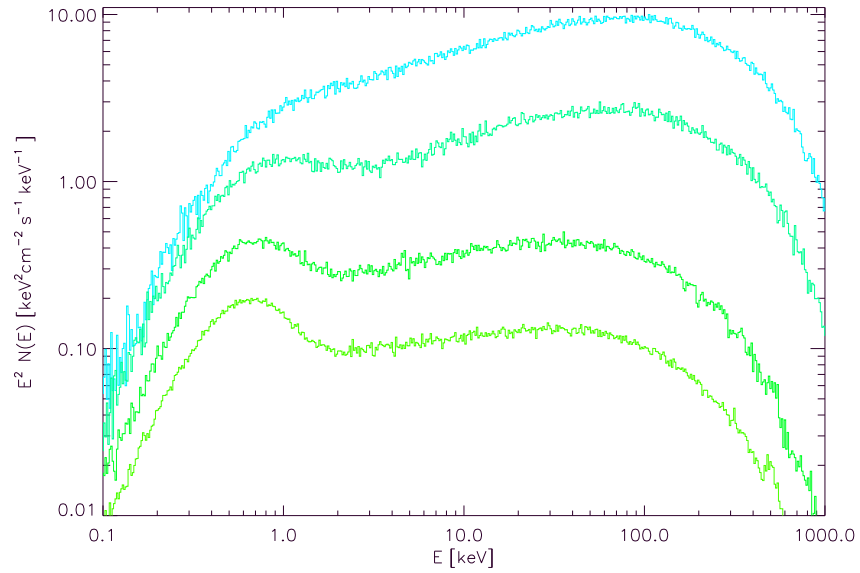


Fig. 5.— The predicted spectrum for various values of the transition layer optical depth. From top to bottom, $\tau_{\text{tr}} = 10, 5, 2.5,$ and 1.0 .

Begelman (1997). The transition layer is treated identically to the corona, except here the heating rate is set to zero. Therefore, the transition layer, numerically modeled using 8 shells, each with equal optical depth $d\tau = \tau_{\text{tr}}/8$, will obtain the Comptonization temperature due to the radiation field from both the corona and the accretion disk.

3.2. Maximum Coronal Temperature

As discussed by Dove, Wilms, & Begelman (1997), for a given total optical depth, there exists a maximum coronal temperature, above which no self-consistent solution exists. Raising the compactness parameter of the corona to a value higher than that corresponding to the maximum temperature gives rise to a higher optical depth (due to pair production), causing more reprocessing, subsequent Compton cooling, and ultimately a *lower* coronal temperature. Here, as much as 80-90% of the incident X-ray flux is re-radiated at the disk temperature, i.e., the X-ray integrated albedo is 0.1-0.2. A completely ionized transition layer will increase the albedo of the cold disk. Accordingly, the amount of energy in the reprocessed blackbody (or Comptonized blackbody) should become smaller with increasing Thomson optical depth of the transition layer, and this Compton cooling via reprocessed radiation should be less efficient and therefore higher maximum coronal temperatures (as compared to models with no transition layer) should be allowed.

In Figure 4, we show how the average coronal temperature varies with the optical depth of the transition layer, τ_{tr} . In Figure 5, we also show the resulting broad band spectra for the model parameters tested. For all models, we chose $l_{\text{bb}} = 0.01$ in order to be consistent with the definition of the disk compactness parameter, i.e., $l_{\text{bb}} \equiv F_{\text{d}}\sigma_{\text{T}}H/(m_{\text{e}}c^3)$, according to which

$$l_{\text{bb}} = 0.03 \left(\frac{\dot{m}}{0.05} \right)^{6/5} (1-f)^{11/10} (\alpha M_1)^{-1/10}. \quad (14)$$

Further, other parameter values are $l_{\text{c}} = 2$, $kT_{\text{bb}} = 150$ keV, and $\tau_{\text{c}} = 0.3$. These parameters correspond to the model producing the maximum coronal temperature. In contrast to models in which $\tau_{\text{tr}} = 0$, the coronal temperature for a given value of τ_{c} is not simply a function of $l_{\text{c}}/l_{\text{bb}}$. To see this, consider the case where $\tau_{\text{tr}} \gg 1$. Here, the albedo of the disk is essentially unity, and therefore all of the soft photons emitted will be from the intrinsic flux of the disk (no reprocessing). Therefore, setting $l_{\text{bb}} \ll 1$ yields the maximum coronal temperatures possible. Note that the maximum temperature levels out as $\tau_{\text{tr}} \rightarrow \infty$. Although, in this limit, there is no reprocessing of hard X-rays in the cold disk, there is still “reprocessing” in the transition layer. As τ_{tr} increases, more coronal radiation is down-scattered to the Compton temperature of the transition layer, which is $kT_{\text{tr}} \sim 1 - 4$ keV. Even at these temperatures, Compton cooling of this “reprocessed” radiation in the corona is very efficient.

It is interesting to note that, only for $\tau_{\text{tr}} \gtrsim 10$, the coronal temperature is high enough such that the corresponding spectrum of escaping radiation is hard enough to describe the observations of Cyg X-1. (The canonical value of the photon power law of Cyg X-1 is $\Gamma = 1.7$; for $\tau_{\text{c}} = 0.3$, this power law corresponds to $kT_{\text{c}} \sim 150$ keV). It is probably unphysical, however, to assume the transition layer is completely ionized for such large optical depths. In fact, the numerical model for $\tau_{\text{tr}} = 10$ predicts a temperature of $kT_{\text{tr}} \sim 500$ eV near the bottom of the layer. Furthermore, as is seen in Figure 6,

the radiation spectra do become substantially softer deeper in the transition layer, and, using our simple experimentation with softer ionizing spectra, shown in Figure 3, we can expect that the gas will become stable and may be at a temperature lower than the Compton temperature for τ_{tr} as small as 2 – 3. Therefore, even with the advent of transition layers, it still appears unlikely that a global slab geometry ADC model can have self-consistent temperatures high enough to reproduce the observed hard spectra of Cyg X-1 and other similar BHCs. This does not rule out ADC models in which the corona is patchy, e.g., containing several localized active regions such as magnetic flares. The patchy geometry leads to higher coronal temperatures due to less reprocessed soft flux re-entering active regions (Poutanen & Svensson 1996), so that lower τ_{tr} may be sufficient to explain the Cyg X-1 spectrum.

3.3. Reprocessing Features in the Spectrum of Escaping Radiation

As shown in Figure 5, the reprocessing features in the spectrum of escaping radiation depend sensitively on the optical depth of the transition layer. In Figure 6, we show how the internal spectrum (averaged over all angles) varies throughout the transition layer and corona. Note that most of the hard X-rays do not penetrate through the transition layer, and that the spectrum gets softer as it approaches the cold disk. On the other hand, the thermal radiation emitted by the disk and the 10-50 keV Compton reflection hump are broadened by Compton scatterings as the disk radiation diffuses upward through the transition layer and the corona. The Iron $K\alpha$ line, small to start with due to the small amount of reprocessing of coronal radiation, is completely smeared out by the time the radiation escapes the system. No line photons are created in the transition layer itself, because we found that the Compton equilibrium state typically resides at the ionization parameter $\xi \gtrsim 10^4$, whereas no fluorescent iron line emission is produced for $\xi \gtrsim 5 \times 10^3$ (Matt, Fabian & Ross 1993, 1996).

Therefore, in agreement with Böttcher, Liang, and Smith (1998), we conclude that a highly ionized transition layer can reduce the reprocessing features in the spectrum of escaping radiation emanating from slab geometry ADC models. Previous work has used the lack of observed reprocessing features to argue against the applicability of slab geometry ADC models, and argued for a disk/corona configuration where the disk has a small solid angle relative to the coronal region, such as a “sphere+disk model (Dove et al. 1998, Gierlinski et al. 1997, Poutanen, Krolik & Ryde 1997). A slab geometry ADC model containing a transition layer, however, is another possibility. Although, as discussed above, these models could not obtain high enough temperatures to be able to predict spectra as hard as the observed spectra of GBHCs unless $\tau_{\text{tr}} \gtrsim 10$, a model with a patchy corona and underlying transition layers appears likely to be able to predict hard enough spectra with a relatively small amount of reprocessing features. In a forthcoming paper, we plan to investigate such a model.

4. DISCUSSION

We have shown that the transition layer in the vicinity of transient flares for ADC models of GBHCs must be highly ionized and very hot. Specifically, due to a thermal instability, the only stable temperature of the transition layer is the local Compton temperature ($kT \sim$ few keV). In fact, even for global ADC models of GBHCs, such a transition layer is found to be likely.

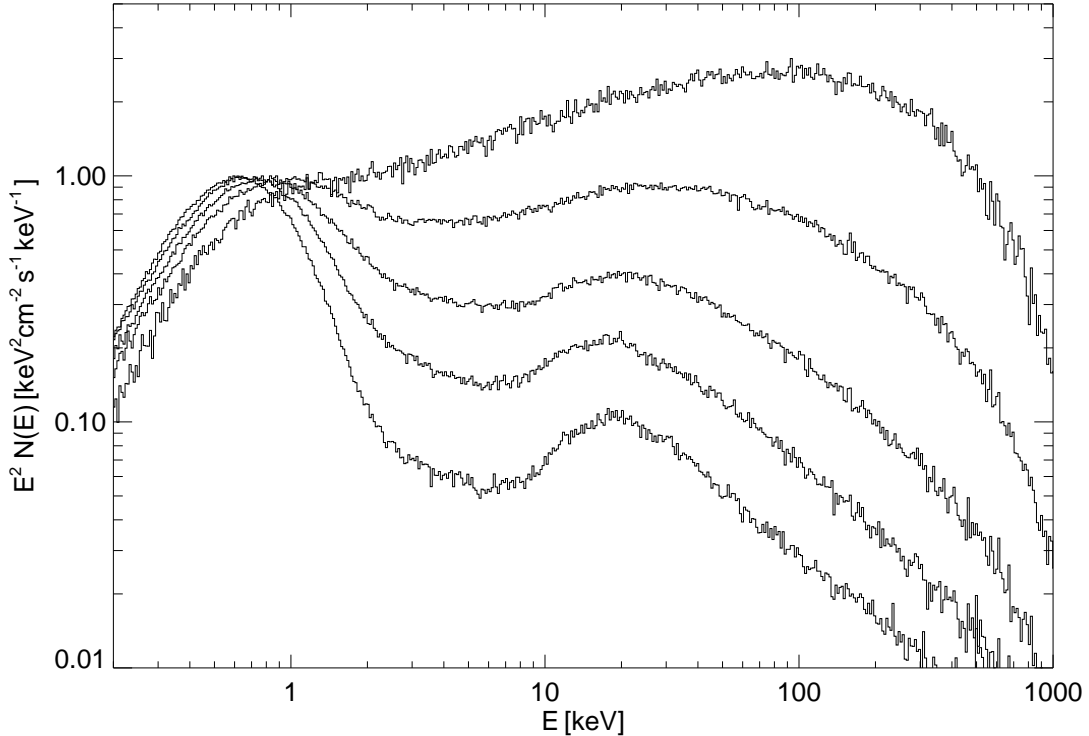


Fig. 6.— Internal spectrum for several shells within the transition disk and corona. From bottom to top, $\tau_{\text{tr}}(z) = 1.25, 2.5, 3.75,$ and 5.0 , where $\tau_{\text{tr}}(z)$ is the Thomson optical depth from the cold-disk/transition layer interface ($z = 0$) to a height z . The uppermost spectrum is the internal spectrum within the corona. For this model, $\tau_{\text{tr}} = 5.0$ and $\tau_c = 0.3$.

However, we have not accurately modeled the full radiative transfer problem through the transition layer at this time, and therefore could not determine its vertical optical depth, which was treated as a free parameter.

Due to the transition layer, a larger fraction of incident X-rays are Compton reflected back into the corona without being reprocessed by the cold disk. In addition, for $\tau_{\text{trans}} \gg 1$, the predicted reprocessing features as well as the thermal excess should be substantially smaller (as is found in this paper for the global ADC model) than that of previous ADC models in which the transition layer was not considered. This reduction of the reprocessing features is crucial for the model being consistent with the observations of GBHCs (e.g., Gierlinski et al. 1997, Dove et al. 1998).

This reduction in reprocessing yields a lower Compton cooling rate within the corona, and higher coronal temperatures than previous ADC models are allowed. For global ADC models with $\tau_c \sim 0.3$, we find that the coronal temperature can be as high as ~ 150 keV if the optical depth of the transition layer is $\tau_{\text{tr}} \gtrsim 10$. However, a completely ionized transition layer with $\tau_{\text{tr}} \gtrsim 10$ is most likely physically inconsistent since the bottom layer was found to be too cold to realistically stay highly ionized. Therefore, global slab-geometry ADC models are still problematic in explaining the observations of GBHCs. Nevertheless, these global ADC results are very encouraging, and a slab geometry ADC model containing a patchy corona (e.g., individual ARs) with underlying transition layers should be rigorously studied. Here, due to the lower amount of reprocessed radiation within the ARs as compared to the global model, models with coronae hot enough to reproduce the observed spectra

of GBHCs may be allowed for more reasonable transition layer optical depths.

We have considered only radiative cooling mechanisms for the transition layer in this paper. It is possible that a wind is induced by the X-ray heating. However, the maximum gas temperature obtained due to the X-ray heating is the Compton temperature ($\lesssim 10^8$ K). Therefore, as shown by Begelman, McKee & Shields (1983), a large scale outflow cannot occur for $R \lesssim 10^4 R_g$. On the other hand, a local uprising of the gas is still possible. The maximum energy flux due to this process is $F_{\text{ev}} \sim P c_s$, where c_s is the sound speed in the transition region. Since $P \lesssim F_x/c$, and $c_s \lesssim 3 \times 10^{-3} c$, we have $F_{\text{ev}}/F_x \lesssim 3 \times 10^{-3}$. Therefore, a wind or any other mechanical process cannot cool the gas efficiently, and thus it is justifiable to consider cooling via emission of radiation only.

In a forthcoming paper, we will discuss the implications of the instability for the case of AGN. As shown in Figures 2 and 3, there is a stable ionization equilibrium state below $T \sim 3 \times 10^5$ Kelvin. Furthermore, due to increasing opacity to the soft disk radiation, we find that equilibria below $T \sim 10^5$ K are not possible. We found that the existence of this stable region, and the unstable region above 3×10^5 K, is very much independent of the details of the incident spectra (indeed, Figures 2 and 3 were not even intended for the AGN case). Thus, it is possible that the differences in the intrinsic X-ray spectra, the ionization state of the reflector and the strength of the iron line in AGNs and GBHCs can be explained by the different end points of the thermal ionization instability described here.

5. ACKNOWLEDGMENTS

SN acknowledges the contributions, guidance and financial support through NASA grant NAG 5-3075 by Prof. Fulvio

Melia. JD acknowledges the useful discussions with P. Maloney, J. Wilms, and M. Nowak.

REFERENCES

- Begelman, M.C., McKee, C.F., & Shields, G.A. 1983, *ApJ*, **271**, 70.
 Böttcher, M., Liang, E. P., & Smith, I. A., 1998, submitted to A&A.
 Brandt, W.N., & Boller, Th. 1998, preprint, astro-ph/9808037
 Dove, J. B., Wilms, J., & Begelman, M. C., 1997, *ApJ*, **487**, 747.
 Dove, J. B., Wilms, J., Nowak, M. A., Vaughan, M. A., 1998, *MNRAS*, **298**, 729.
 Field, G.B. 1965, *ApJ*, **142**, 531.
 Galeev, A. A., Rosner, R., & Vaiana, G. S., 1979, *ApJ*, **229**, 318.
 Gierlinski, M. et al. 1997, *MNRAS*, **288**, 958.
 Haardt, F., & Maraschi, L. 1991, *ApJ*, **380**, L51.
 Haardt, F., & Maraschi, L. 1993, *ApJ*, **413**, 507.
 Haardt, F., Maraschi, L., & Ghisellini, G. 1994, *ApJ*, **432**, L95.
 Kallman, T. R., & McCray, R. 1982, *ApJS*, 50, 263
 Kallman, T.R., & Krolik, J.H., 1986, NASA/GSFC Laboratory for High Energy Astrophysics special report.
 Krolik, J.H., McKee, C.F., & Tarter, C.B. 1981, *ApJ*, **249**, 422.
 Maciolek-Niedzwiecki, A., Krolik, J.H., & Zdziarski, A.A. 1997, *ApJ*, **483**, 111.
 Magdziarz, P. & Zdziarski, A.A. 1995, *MNRAS*, **273**, 837.
 Matt, G., Fabian, A.C., & Ross, R. R. 1993, *MNRAS*, **262**, 179.
 Matt, G., Fabian, A.C., & Ross, R. R. 1996, *MNRAS*, **278**, 1111.
 Nayakshin, S. & Melia, F. 1997, *ApJL*, **484**, L103.
 Nayakshin S. 1998, Ph.D. Thesis, The University of Arizona. Also available on astro-ph archive.
 Nandra, K. & Pounds, K. 1994, *MNRAS*, **268**, 405.
 Pounds, K.A. et al. 1990, *Nature*, **344**, 132.
 Poutanen, J., Nagendra, K.N., & Svensson, R. 1996, *MNRAS*, **283**, 892.
 Poutanen, J. & Svensson, R. 1996, *ApJ*, **470**, 249.
 Poutanen, J., Krolik, J.H. & Ryde, F. 1997, in the Proceedings of the 4th Compton Symposium, astro-ph/9707244
 Poutanen, J., Svensson, R., & Stern, B. 1997, in the Proceedings of the 2nd INTEGRAL Workshop "The Transparent Universe", ESA SP-382,
 Ross, R.R., Fabian, A.C., & Brandt, W.N. 1996, *MNRAS*, **278**, 1082.
 Sincell, M.W. & Krolik, J.H. 1997, *ApJ*, **476**, 605S.
 Stern, B., Poutanen, J., Svensson, R., Sikora, M., & Begelman, M. C. 1995, *ApJ*, **449**, L13.
 Svensson, R. & Zdziarski, A. 1994, *ApJ*, **436**, 599.
 Svensson, R. 1996, A&AS, 120, 475
 Zdziarski, A.A. et al. 1996, A&AS, 120, 553
 Życki, P.T. et. al. 1994, *ApJ*, **437**, 597.